



Featuring work from the King and Bashir groups at the University of Illinois Urbana-Champaign and the work of Advanced Diamond Technologies.

Title: Rapid thermal lysis of cells using silicon–diamond microcantilever heaters

Rapid lysis of single cells and bacteria is demonstrated using local heating from silicon–diamond microcantilevers with integrated solid state resistive heaters.

As featured in:



See Bashir, King *et al.*, *Lab Chip*, 2010, **10**, 1135–1141

Rapid thermal lysis of cells using silicon–diamond microcantilever heaters†

Natalya Privorotskaya,^{‡a} Yi-Shao Liu,^{‡b} Jungchul Lee,^a Hongjun Zeng,^e John A. Carlisle,^e Adarsh Radadia,^{bd} Larry Millet,^{bd} Rashid Bashir^{bcd} and William P. King^{*ad}

Received 11th November 2009, Accepted 25th January 2010

First published as an Advance Article on the web 12th March 2010

DOI: 10.1039/b923791g

This paper presents the design and application of microcantilever heaters for biochemical applications. Thermal lysis of biological cells was demonstrated as a specific example. The microcantilever heaters, fabricated from selectively doped single crystal silicon, provide local resistive heating with highly uniform temperature distribution across the cantilevers. Very importantly, the microcantilever heaters were coated with a layer of 100 nm thick electrically insulating ultrananocrystalline diamond (UNCD) layer used for cell immobilization on the cantilever surface. Fibroblast cells or bacterial cells were immobilized on the UNCD/cantilever surfaces and thermal lysis was demonstrated *via* optical fluorescence microscopy. Upon electrical heating of the cantilever structures to 93 °C for 30 seconds, fibroblast cell and nuclear membrane were compromised and the cells were lysed. Over 90% of viable bacteria were also lysed after 15 seconds of heating at 93 °C. This work demonstrates the utility of silicon–UNCD heated microcantilevers for rapid cell lysis and forms the basis for other rapid and localized temperature-regulated microbiological experiments in cantilever-based lab on chip applications.

Introduction

Microcantilever sensors can be very useful in micro-systems based bioanalytical tools, where they can potentially be used as sensing elements in applications such as detection of DNA hybridization,^{1–4} capture of bacteria or viruses,^{5,6} or characterization of single adherent cells in fluids in a non-invasive manner.⁷ Integration of additional functionality such as localized heating on the microcantilevers is also highly desirable. Such microcantilevers with integrated resistive heaters have the advantage of locally controlling temperature in both air and liquid environments and have the potential for use in many biochemical applications.^{8–10} Local temperature control could enable improved sample preparation, compatible with the use of smaller sample sizes, and help to realize many novel biological investigations beyond conventional technologies, especially for temperature-mediated biological reactions, such as enzyme reactions, DNA hybridization and cell lysis.

Heat-mediated lysis of cells is a simple and effective method for DNA extraction^{11,12} and is required for many biotechnological methods including Southern blotting and polymerase chain reaction (PCR).^{13,14} However, due to heat transfer efficiency in conventional samples, long incubation time (10 minutes,

90–100 °C) is required for efficient DNA extraction from cells suspended in a centrifuge tube.¹⁵ Currently available smaller microfluidic devices usually utilize an electrical or a mechanical lysis approach and may require up to several minutes to complete the cell lysis procedure.^{16,17} Integrated heating and cell lysis would be a very desirable function in microfluidic lab on chip devices, especially where cantilevers are used as sensing or processing elements. Cantilevers with rapid and precise thermal control could offer significant improvements over current approaches, and potentially can be used to release DNA and RNA from single to just a few mammalian cells for processing and sensing. The lysed material can be collected if the cantilevers were positioned in a microfluidic channel and if a flow was used during or right after heating the cantilever heaters.

Microcantilevers fabricated from doped single crystal silicon can be engineered to have regions of highly uniform temperature, with temperature that can be calibrated and controlled to above 250 °C.⁸ For such a cantilever to be operated in a liquid for biochemical analysis, it is critical that the cantilevers be passivated with an insulating material which promotes adhesion of biological entities such as cells. In addition, the insulating material should be free of pinholes and defects and should not allow current flow through it when electrically operated in conductive solutions. A novel alternative to the typically used silicon oxide or silicon nitride passivation films is chemical vapor deposited (CVD) ultrananocrystalline diamond (UNCD), which has been shown to be superior to silicon for cell attachment and biochemical stability.^{18,19} Additionally, UNCD can be deposited on silicon microcantilevers²⁰ and with a high degree of electrical isolation,²¹ allowing the silicon cantilevers to be used as heaters in conductive solutions.

To maximize the utility of thermally controlled cantilevers, we incorporated UNCD onto silicon cantilevers to provide a stable chemical surface, thus providing for a well-characterized and

^aDepartment of Mechanical Science and Engineering, University of Illinois Urbana-Champaign, USA. E-mail: wpk@illinois.edu

^bDepartment of Electrical and Computer Engineering, University of Illinois Urbana-Champaign, USA. E-mail: rbashir@illinois.edu

^cDepartment of Bioengineering, University of Illinois Urbana-Champaign, USA

^dMicro and Nanotechnology Laboratory, University of Illinois Urbana-Champaign, USA

^eAdvanced Diamond Technologies, Inc., Romeoville, IL, USA

† Electronic supplementary information (ESI) available: Finite element simulations and additional microscopy. See DOI: 10.1039/b923791g

‡ Authors contributed equally.

highly uniform temperature distribution and improved cell attachment. We describe heated silicon–UNCD composite microcantilevers designed to have large regions of highly uniform temperature. These cantilevers offer the integrated heating characteristics of silicon with the stability and biological compatibility of diamond. Our study demonstrates that Si–UNCD cantilevers provide a highly localized heating platform with high efficiency heat-transfer that induces cell lysis within 30 seconds at a temperature of approximately 93 °C.

Materials and methods

Device design and fabrication

Fig. 1(a) shows a schematic of a silicon cantilever having an integrated resistive heater⁸ and a 100 nm thick coating of

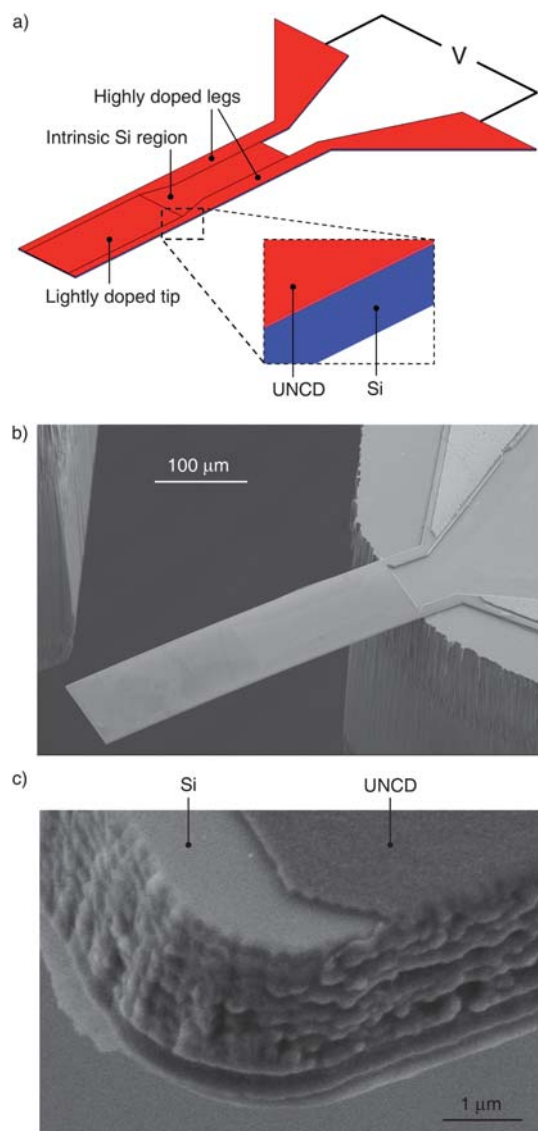


Fig. 1 (a) Schematic of a Si–UNCD cantilever. The cantilever is 400 μm long and 100 μm wide with 100 nm of UNCD coating on top of 2 μm thick Si. (b) SEM image of a fabricated Si–UNCD hotplate cantilever. (c) Close-up view of the cantilever corner showing the 2 μm thick silicon cantilever with 100 nm UNCD coating.

undoped UNCD. The diamond layer on the cantilever provides a biocompatible and electrically isolated layer on the heating element. Fig. 1(b) shows a scanning electron micrograph (SEM) of a fabricated cantilever with a detailed view of the 100 nm UNCD coating on the silicon layer shown in Fig. 1(c). The light grey region at the cantilever base corresponds to the location and geometry of intrinsic silicon seen through the UNCD layer. Slight cantilever bending was observed due to the thermal mismatch at the Si–UNCD boundary.

Fig. 2 shows the key steps in the fabrication process. Fabrication began with a silicon-on-insulator wafer consisting of a 400 μm silicon handle layer, 1 μm buried oxide layer, and 2 μm silicon device layer. First, the device layer was patterned and etched using an inductively coupled plasma (ICP) etcher to define the cantilever geometry (Fig. 2(a)). The silicon cantilever was then selectively doped with phosphorus to form resistive heating regions and highly conductive current paths (Fig. 2(b and c)). The device was annealed at 1000 °C for 2 hours after each implantation step to diffuse and activate the dopant. Electrically conducting traces (10²⁰ cm⁻³) were patterned along the sides of the cantilever, while a resistive heater (10¹⁷ cm⁻³) was patterned near the cantilever free end. The shapes of the doped silicon regions were optimized to maximize the cantilever temperature uniformity.⁸ Next, a 100 nm thick UNCD layer was grown over the entire cantilever structure to produce conformal insulating diamond coating. UNCD was etched in oxygen plasma with

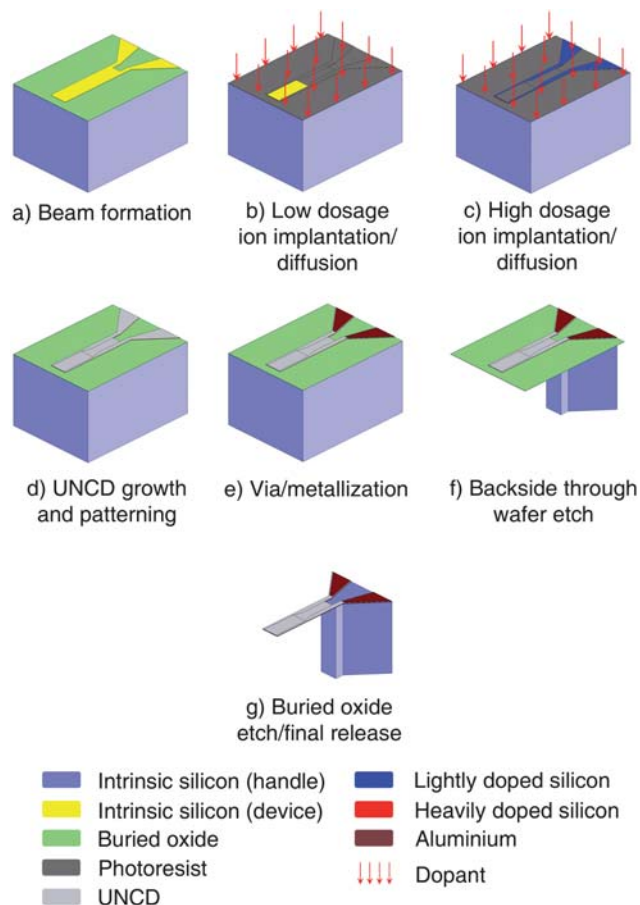


Fig. 2 Major steps in the fabrication of Si–UNCD cantilevers.

silicon dioxide as a mask to the same dimensions as the silicon cantilever defined in step (a). Contact openings were made in the same fashion. Aluminium evaporation and wet etching defined electrical contacts to the cantilever (Fig. 2(e)). Annealing the device at 400 °C for 30 minutes after metal deposition promoted aluminium adhesion to UNCD. Cantilevers were released *via* through wafer etching from the backside, followed by a short dip into 49% HF to remove any exposed silicon dioxide.

Cantilever characterization

The electrical and thermal characteristics of the cantilever were determined using well-characterized processes.⁹ Fig. 3(a) shows cantilever electrical resistance and dissipated power for a given voltage applied to the cantilever when operated in series with a 5 kΩ resistor. The cantilever electrical resistance increases over the entire voltage range due to the decrease in carrier mobility at elevated temperature.²² The cantilever heater temperature was measured as a function of the cantilever heating power using Raman spectroscopy.²³ The UNCD was transparent to our Raman laser and because of its thickness was assumed to be the same temperature as the silicon heater because of its small thickness. Fig. 3(b) shows measured temperature distribution comprised of 95 data points on a 20 μm × 25 μm grid across the cantilever at three different heating powers. The cantilever temperature is close to room temperature at the cantilever base and is highest at the cantilever free end. The temperature uniformity, defined as standard deviation with respect to the average temperature, is better than 5% over 100 μm of the device length at the free end as indicated in Fig. 3(c). The addition of the diamond layer to the cantilever does not have a significant effect on temperature variation over cantilever length as compared to purely silicon cantilevers, as the thermal conductivity of UNCD is low compared to silicon and the UNCD layer is very thin.²⁴ At the highest measured power, the Si–UNCD cantilever is capable of heating to above 400 °C, which is 62% higher than in a comparable silicon device.⁸

Temperature increase in the surrounding medium due to the resistive heating of the cantilever was characterized based on ANSYS electro-thermal simulation, which included cantilever immersion in 20 μl of solution. The results of the simulation are shown in Fig. S1(a) of the ESI† with Fig. S1(b) providing a close-up view of the cantilever region. A cross-section through the fluid is taken 50 μm from the free end of the cantilever for temperature visualization. Only 5 nl of solution directly in contact with the cantilever heats up to within 20% of the lysis target temperature of 93 °C. Thus, when the heat lysis experiment is carried out, the monolayer of cells attached to the cantilever surface is expected to be at a temperature close to that of the cantilever itself, while the rest of the solution would be at much lower temperatures.

Surface treatments for mammalian and bacterial cell attachment

The Si–UNCD cantilever was attached and wire-bonded in a well of dual-inline package (DIP). The contact pads of the cantilever were covered by torr-sealant (Varian, Inc., Palo Alto, CA 94304, USA). The Si–UNCD cantilever was exposed in the well formed by the cavity of the dual-line package and torr-sealant. The total volume of the well could accommodate a 20 μl sample.

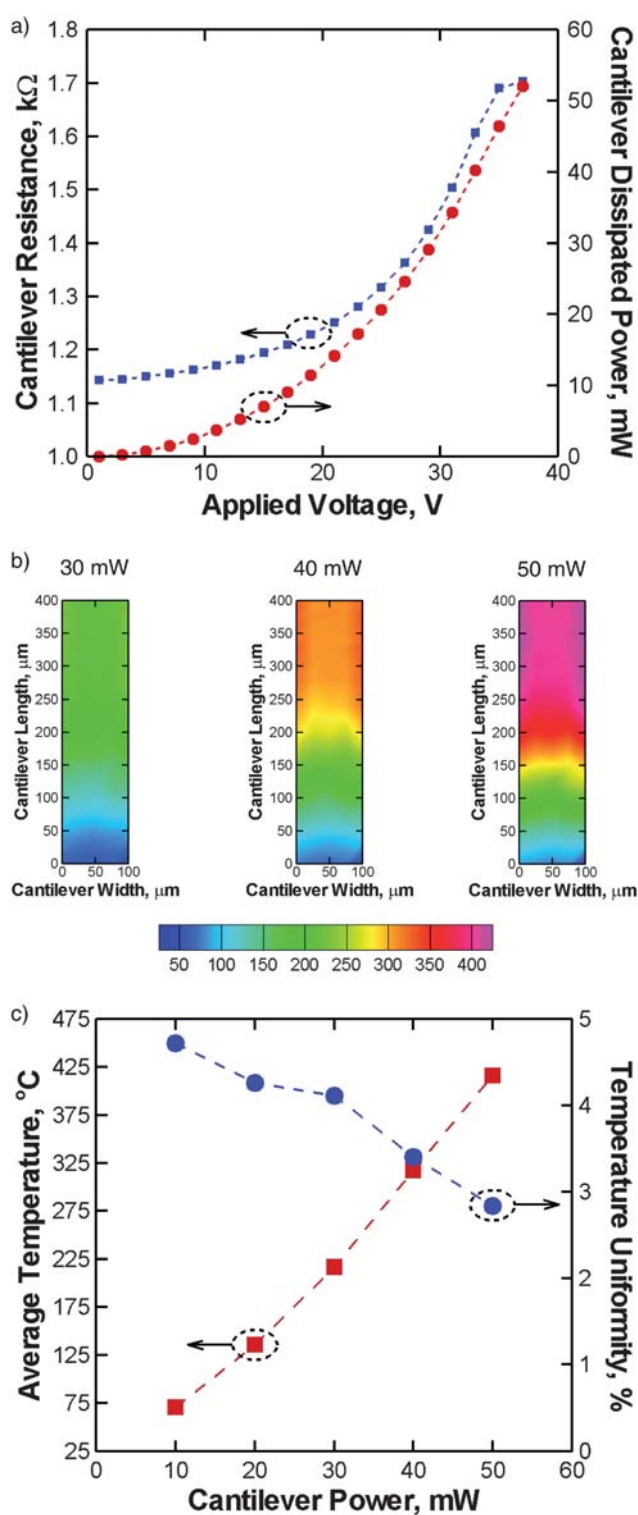


Fig. 3 (a) Electrical characterization of the heated Si–UNCD hotplate cantilever. Cantilever electrical resistance and dissipated power are measured as a function of applied voltage to the thermal runaway point. The measurements are made with a 5 kΩ resistor in series with the cantilever. (b) Temperature distribution at various dissipated powers obtained using Raman spectroscopy. (c) Average temperature and temperature uniformity within 100 μm square region at the cantilever end. Temperature variation is measured as standard deviation in this region.

The device was exposed to UV-light and sterilized for at least 12 hours before the biological experiments. PBS (with calcium and magnesium) was used to wash the device three times after the sterilization. To enhance mammalian cell attachment, the devices were first washed with PBS (0.01 M Na₂HPO₄, 0.01 M NaH₂PO₄, and 0.5 M NaCl, pH 7.4) and then poly-L-lysine (0.01%, Sigma-Aldrich, Inc., St Louis, MO 63103, USA) was used to coat the UNCD surface (2 hours) before cell attachment. This process enhanced the number of cells attached to the surface and also improved cell adhesion. To improve bacterial cell attachment, we immobilized *Listeria monocytogenes* V7 on the Si-UNCD cantilever *via* Hsp60. Biotinylated bovine serum albumin (B-BSA, Sigma-Aldrich, Inc., St Louis, MO 63103, USA) at 2 mg ml⁻¹ in PBS was first added to the device and incubated at ambient temperature for 30 minutes. After washing the device twice with 0.5% Tween 20 in PBS (PBS-T) and once with PBS, streptavidin (from *Streptomyces avidinii*, 1 mg ml⁻¹, Sigma-Aldrich, Inc., St Louis, MO 63103, USA) was incubated on the device at ambient temperature for 15 minutes. Excess streptavidin was removed by washing with PBS-T and PBS (same as previous washing step). The device was then incubated with biotinylated-Hsp60 (1 μg ml⁻¹) for 1 hour at ambient temperature, followed by washing steps with PBS-T and PBS.²⁵ Purified recombinant Hsp60 from human promyelocytic leukemia cells (HL-60) was purchased from Assay Design (Ann Arbor, MI). Sulfo-NHS-LC conjugated biotin (10 mM; Pierce, Rockford, IL) was prepared in deionized (DI) water and conjugated to the primary amine group of Hsp60 for biotinylation according to the manufacturer's instructions.

Cells, either NIH 3T3 fibroblast (ATCC, Manassas, VA) or *L. monocytogenes* V7 (Food Science Department, Purdue University, West Lafayette, Indiana), were then fluorescently labeled, introduced, and incubated on the device and were ready for heat-mediated lysis experiments. (The sample, 20 μl, was added into the well by pipetting in a biosafety level 2 (BSL 2) hood. The microcantilever heater was totally submerged in the 20 μl sample. The device (DIP package) was kept in a sterilized Petri dish throughout the UV sterilization, cell loading, incubation, and attachment steps.)

Mammalian cell culture and preparation

NIH 3T3 fibroblast cells were used in this study and were cultured in Eagle's medium with α modification (Sigma-Aldrich, Inc., St Louis, MO 63103, USA), supplemented with 10% FBS (Sigma-Aldrich, Inc., St Louis, MO 63103, USA), 4 mM L-glutamine (Invitrogen, Carlsbad, CA, 92008, USA) and antibiotics (penicillin, 1000 IU ml⁻¹ and streptomycin, 1000 μg ml⁻¹) (Invitrogen Corporation, Carlsbad, CA 92008, USA) at 37 °C with 5% CO₂, 100% humidity in a mammalian culture incubator. The initial seeding density was 10⁵ cells ml⁻¹ in 5 ml culture medium in a 25 ml flask. After incubating for 3 days, the cells reached a population of 10⁶ cells in the 25 ml flask and were harvested for experiment. Cells were detached from the flask surface by first removing the culture medium from the flask and then washing with pre-warmed (37 °C) phosphate buffered saline (PBS, without calcium and magnesium, Lonza Walkersville, Inc., MD 21793, USA) to ensure that there was no culture medium remaining in the flask. Pre-warmed trypsin-EDTA (0.25%

trypsin-0.53 mM EDTA in HBSS without calcium and magnesium, ATCC, Manassas, VA 20110, USA) was then introduced into the flask, 2 ml in 25 ml flask. The flask was gently agitated to have a uniform coverage of trypsin-EDTA and then incubated at 37 °C for 5 minutes. After enzyme incubation, 3 ml medium was aspirated into the flask to inhibit trypsin-EDTA from further damaging the cells. Cell viability was examined by staining cells with trypan blue²⁶ and cells were counted using a hemocytometer on an inverted light microscope. Cells were introduced into the well of the DIP device at a final concentration of 10⁵ cells ml⁻¹.

L. monocytogenes culture and preparation

L. monocytogenes V7 were incubated in Luria Bertani (LB) (Lennox, Fisher Scientific, New Jersey 07410, USA) medium at 37 °C and harvested at 16 hours after inoculation to guarantee a high percentage of live cell population. The concentration of the sample was ~10⁷ cfu ml⁻¹ (counted by agar plating) and was further concentrated 10 times by centrifugation and re-suspension in LB medium. The viability of the bacteria was confirmed by DiOC₆(3) (AnaSpec Inc., San Jose, CA 95131, USA), Hoechst 33258 (Fluka, Sigma-Aldrich, Inc., St Louis, MO 63103, USA), and propidium iodide (PI) (Fluka, Sigma-Aldrich, Inc., St Louis, MO 63103, USA), which were also used as the live-dead assay to verify the membrane integrity after heat lysis experiments. Samples with a concentration of live cells over 80% were used for experiments.

Fluorescent dyes used for live-dead assay

Cell membrane integrity was examined with propidium iodide (PI), which can only penetrate through compromised cell membrane and bind to DNA by intercalating between the bases. Once PI dye is bound to nucleic acids, its fluorescence is enhanced 20 to 30 fold and is commonly used for identifying dead cells in a population. DiOC₆(3) and Hoechst 33258 were also used as indicators for cell locations and controls. Hoechst 33258 is a DNA labeling fluorescent dye that can permeate into intact cells and can be used on live or membrane-compromised cells. DiOC₆(3) is a fluorescent dye generally used for staining live cells by binding to mammalian cells' endoplasmic reticulum, vesicle membranes, mitochondria, and to bacteria's lipid bilayer due to a potential across the plasma membrane.²⁵ The staining procedures were optimized and developed based on the staining protocols provided by Invitrogen™ and previous literature.²⁷⁻³⁰ The final concentrations of PI, DiOC₆(3), and Hoechst 33258 used in the mammalian cells lysis experiments were 2 μg ml⁻¹, 15 μg ml⁻¹, and 20 μg ml⁻¹, respectively. In the bacteria lysis experiments, the final concentrations of PI, DiOC₆(3), and Hoechst 33258 were 2 μg ml⁻¹, 12 μg ml⁻¹, and 25 μg ml⁻¹ respectively.

Fixation of cells for SEM imaging

Cells were fixed with 2% paraformaldehyde (methanol-free, ultra pure EM grade), 2.5% glutaraldehyde (EM grade), and 0.1 M Na-cacodylate buffer, pH 7.4 (cacodylic acid, sodium salt solution) (all fixation chemicals were from Polyscience, Inc., Warrington, PA 18976, USA) at 4 °C for 4 hours. Fixed cells were then washed with 0.1 M Na-cacodylate buffer for 10 minutes on

a shaker table followed by 37%, 67%, and 95% ethanol wash, each for 10 minutes, on a shaker table. The final washing step includes a 100% ethanol wash, 3 times, 10 minutes each, on a shaker table. The device with fixed cells was stored in 100% ethanol at 4 °C, then dried with a critical point dryer and coated with gold/palladium prior to SEM imaging.

Results and discussion

Mammalian cell lysis

NIH 3T3 fibroblast cells were cultured and prepared as described above. Cells were stained with DiOC₆(3) (final concentration 15 μg ml⁻¹) and Hoechst 33258 (final concentration 20 μg ml⁻¹) to show the condition of the cell membrane and its nucleus. PI (final concentration 2 μg ml⁻¹) was also added to the solution as an indicator of compromised cell membrane, which is observed when heat creates holes through which PI can penetrate the membrane and stain DNA and RNA. Cells were added and incubated with poly-L-lysine coated cantilever at 37 °C, 5% CO₂, with 100% humidity in a mammalian culture incubator. Cells were attached and spread on the cantilever during 2 hours incubation, as shown in Fig. 4(a and b).

Once the cells were attached, they were examined with a microscope under bright field as shown in the left image of Fig. 4(c). Cells appear round and healthy and their viability was further confirmed with fluorescence before cantilever heating, as shown in the first row of Fig. 4(d). The green images show the

cells labeled with DiOC₆(3) dye which labels the lipid membrane, the blue images show the labeling of the nucleic acid molecules using the Hoechst dye indicating the presence of DNA, and the red images show the red propidium iodide stain indicating that the two cells on the upper left were compromised before the cantilever was heated, while the other two cells with the solid arrows were healthy. The intensity of the Hoechst dye in these cells was high and localized in a region within the cells, thus indicating that the nuclear membrane was still intact and the nucleic acid molecules were confined within the nucleus, whereas in the two cells with compromised membranes, the nucleic acid molecules were diffused throughout the cell as indicated by the cell area (green dye) being about the same as the nuclear area (blue dye).

The cantilever was heated to 93 °C with applied voltage of 23 V corresponding to 17 mW of dissipated power as pre-calibrated by Raman spectroscopy (Fig. 3(a and c)). The integrity of the cell membrane of the cell located at the cantilever free end was compromised after heating the cantilever for 20 seconds as evident from the additional staining of its nucleus with PI dye in the middle-right panel in Fig. 4(d). However, at this point in the experiment, both PI and Hoechst dyes were restricted to the nucleus showing that the cell had not been completely lysed. After heating the cantilever for an additional 10 seconds, the propidium iodide dye became visible at all cell locations as shown in the bottom row of Fig. 4(d), indicating that all of the membranes were compromised. No clear intact cell membrane was observed in the bright field image in the right panel of

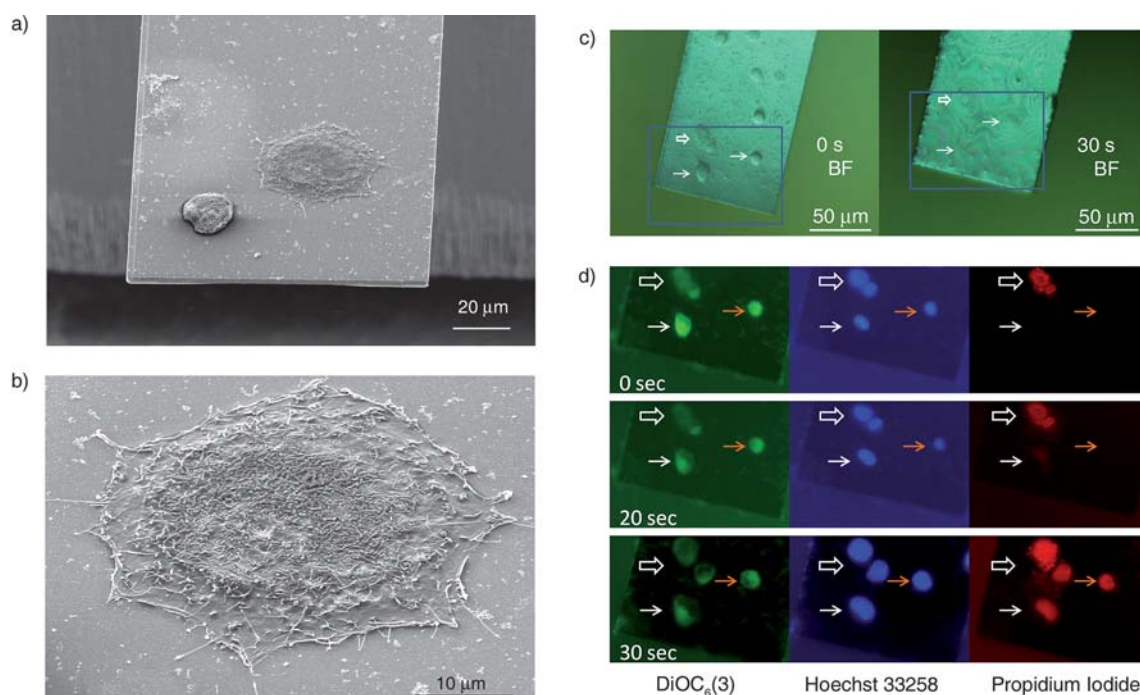


Fig. 4 (a) SEM image of NIH 3T3 fibroblast cells on a hotplate Si-UNCD cantilever. (b) A close-up view of a cell attached and spread on the UNCD surface. (c) NIH 3T3 fibroblast cells grown on the UNCD cantilever before (left) and after heat lysis at 93 °C for 30 seconds (right). The cells are not visible in bright field after the heat lysis, however, they are clearly visible when fluorescent markers are used. (d) Fluorescent images of the same regions as shown in (c). The hollow arrows indicate two cells were dead from the beginning of the experiment; solid arrows show a progressive cell death during heat lysis. The cell membrane of one of the healthy cells at the beginning of the experiment started to become compromised after 20 seconds of heating. The orange solid arrows show another healthy cell subsequently lysed at 30 seconds of heating. DiOC₆(3) labels cell lipid membrane, Hoechst labels cell DNA, and propidium iodide is incorporated into dead cells.

Fig. 4(c) after the experiment. The nuclear membrane of all the cells was also lysed due to heating, as shown in the bottom row of Fig. 4(d), where Hoechst and PI dyes were diffused throughout the cell. Co-localizations of various fluorescent stains before and after heat lysis were further illustrated with overlaid images of R (red), G (green), and B (blue) channels (ESI†, Fig. S2). Because the temperature of the cantilever at the device free end is constant within 5% as shown in Fig. 3(b and c) and surface cell coverage is limited to a monolayer or less, cell density is not expected to affect the thermal-lysis efficiency.

Bacteria lysis

In addition to the mammalian cells, the heat-lysis assay was also applied to bacteria cells. Fig. S3(a and b) in the ESI† show SEM images of *L. monocytogenes* V7 on the Si-UNCD cantilever. The bacteria cells were first stained and incubated at 37 °C with Hoechst 33258 (25 µg ml⁻¹) for 10 minutes, followed by 10 minutes with propidium iodide (2 µg ml⁻¹) and 10 minutes with DiOC₆(3) (12 µg ml⁻¹). The bacteria cells were added and incubated with the Hsp60-functionalized cantilever for the heat-lysis experiment at 37 °C for 1 hour.

Before electrically heating the cantilever, the viability of the bacterial cells was confirmed on the cantilever with fluorescent microscope. As shown in Fig. 5(a), only about 8.5% of the cells were dead or had their membranes compromised (top right-most panel in Fig. 5(a and c)) and over 90% of the cells were healthy under the green and blue filters, as indicated by the lack of penetration of propidium iodide. The cantilever was heated at 93 °C for 15 seconds with an applied voltage of 23 V. Fig. 5(b and c)

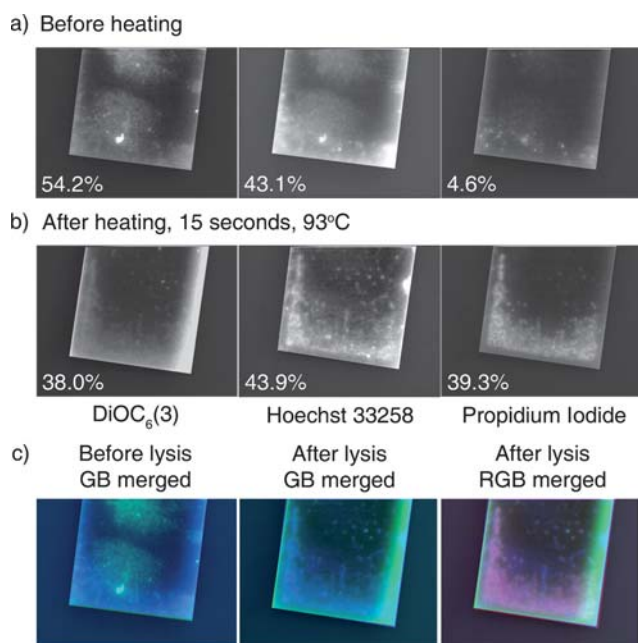


Fig. 5 Heat lysis of *L. monocytogenes* V7 on a Si-UNCD hotplate cantilever: (a) grey scale images taken before applying heat and (b) grey scale images taken after experiment with heating at 93 °C for 15 seconds. DiOC₆(3) labels cell lipid membrane, Hoechst labels cell DNA, and propidium iodide is incorporated into dead cells. Percentages indicate the fraction of cantilever area covered by bacteria. (c) Merged data for bacterial lysis before and after cantilever heating.

show the images of bacteria cells taken after the heat treatment. The ratio of live vs. dead was calculated from the percentage of areas covered with cells labeled by propidium iodide and DiOC₆(3) respectively. The percentage of areas was processed and calculated with auto-threshold by ImageJ (National Institute of Health), except cells labeled with propidium iodide before heat treatment, in which only a few cells were labeled and could not be picked up exclusively by auto-threshold. As shown in Fig. 5, all of the cells on the cantilever are compromised, with either all or some of their membranes lysed, due to the electrical heating as indicated by the penetration of the propidium iodide dye in the cells and the co-location of the membrane dye and the nucleic acid dye. In comparison, for the images before heating, only 8.5% of the bacteria cells were initially dead as observed under a fluorescence microscope with a Tex Red filter and quantified *via* ImageJ. These results clearly indicate that the membranes of the bacteria were lysed due to the application of the high temperature on the cantilever.

Control experiments were carried out at the same time without heating (data not shown). Cells, both NIH 3T3 fibroblast and *L. monocytogenes*, could survive a few hours after experiments took place. Cells could further attach and grow on the cantilevers for periods of 12–24 hours.⁷

Conclusion

Heat mediated cell-lysis is required for many biochemical assays, especially in applications requiring a simple way of releasing cell content, such as chromosomes, RNA, and DNA. Lysing cells on a micro-fabricated Si-UNCD cantilever provides an efficient and target-specific lysis platform for releasing the cell components when combined with surface chemistry immobilization or microfluidics. As can be seen from Fig. 4 and 5, DNA molecules (stained by Hoechst and PI dyes) were still on the cantilever during the lysis process and could be used for downstream application using the heating cantilever, such as PCR. Incorporation of the devices in a microfluidic channel and collection of the lysate from a flow would allow the downstream detection of the molecules from the cells.

As shown in this study, the rapid heat-transfer through the Si-UNCD cantilever compromised the membranes of NIH 3T3 fibroblasts and lysed the cell nuclei within 30 seconds. Bacteria cells, *L. monocytogenes* V7, were shown to be lysed within 15 seconds. The rapid and localized heating on the cantilevers themselves make these devices very attractive for a variety of biochemical analyses and assays.

Acknowledgements

This research was supported through the Defense Threat Reduction Agency, a cooperative agreement with the Agricultural Research Service of the US Department of Agriculture, project number 1935-4200-035, and the Center for Food Safety and Engineering at Purdue University.

References

- 1 N. V. Lavrik, M. J. Sepaniak and P. G. Datskos, *Rev. Sci. Instrum.*, 2004, **75**, 2229–2253.
- 2 C. Ziegler, *Anal. Bioanal. Chem.*, 2004, **379**, 946–959.

- 3 T. Thundat, P. I. Oden and R. J. Warmack, *Microscale Thermophys. Eng.*, 1997, **1**, 185–199.
- 4 A. Boisen and T. Thundat, *Mater. Today (Oxford, U. K.)*, 2009, **12**, 32–38.
- 5 B. Ilic, D. Czaplewski, H. G. Craighead, P. Neuzil, C. Campagnolo and C. Batt, *Appl. Phys. Lett.*, 2000, **77**, 450–452.
- 6 A. Gupta, P. Nair, D. Akin, S. Broyles, M. Ladisch, A. Alam and R. Bashir, *Proc. Natl. Acad. Sci. U. S. A.*, 2006, **103**, 13362–13367.
- 7 K. Park, J. Jang, D. Irimia, J. Sturgis, J. Lee, J. P. Robinson, M. Toner and R. Bashir, *Lab Chip*, 2008, **8**, 1034–1041.
- 8 N. L. Privorotskaya and W. P. King, *Sens. Actuators, A*, 2009, **152**, 160–167.
- 9 J. Lee and W. P. King, *J. Microelectromech. Syst.*, 2008, **17**, 432–445.
- 10 J. Lee and W. P. King, *IEEE Sens. J.*, 2008, **8**, 1805–1806.
- 11 J. Membrillo-Hernandez, A. Nunez-de la Mora, T. del Rio-Albrechtsen, R. Camacho-Carranza and M. C. Gomez-Eichelmann, *J. Basic Microbiol.*, 1995, **35**, 41–46.
- 12 D. S. Holmes and M. Quigley, *Anal. Biochem.*, 1981, **114**, 193–197.
- 13 E. M. Southern, *J. Mol. Biol.*, 1975, **98**, 503–517.
- 14 R. K. Saiki, D. H. Gelfand, S. Stoffel, S. J. Scharf, R. Higuchi, G. T. Horn, K. B. Mullis and H. A. Erlich, *Science*, 1988, **239**, 487–491.
- 15 E. Padilla, V. González, J. M. Manterola, J. Lonca, A. Perez, L. Matas, M. D. Quesada and V. Ausina, *Diagn. Microbiol. Infect. Dis.*, 2003, **46**, 19–23.
- 16 J. T. Nevill, R. Cooper, M. Dueck, D. N. Breslauer and L. P. Lee, *Lab Chip*, 2007, **7**, 1689–1695.
- 17 D. Di Carlo, K.-H. Jeong and L. P. Lee, *Lab Chip*, 2003, **3**, 287–291.
- 18 P. Bajaj, D. Akin, A. Gupta, D. Sherman, B. Shi, O. Auciello and R. Bashir, *Biomed. Microdevices*, 2007, **9**, 787–794.
- 19 W. Yang, O. Auciello, J. E. Butler, W. Cai, J. A. Carlisle, J. E. Gerbi, D. M. Gruen, T. Knickerbocker, T. L. Lasseter, J. N. Russell, Jr, L. M. Smith and R. J. Hamers, *Nat. Mater.*, 2002, **1**, 253–257.
- 20 X. Xiao, J. Birrell, J. E. Gerbi, O. Auciello and J. A. Carlisle, *J. Appl. Phys.*, 2004, **96**, 2232–2239.
- 21 A. R. Krauss, O. Auciello, D. M. Gruen, A. Jayatissa, A. Sumant, J. Tucek, D. C. Mancini, N. Moldovan, A. Erdemir, D. Ersoy, M. N. Gardos, H. G. Busmann, E. M. Meyer and M. Q. Ding, *Diamond Relat. Mater.*, 2001, **10**, 1952–1961.
- 22 R. F. Pierret, *Semiconductor Device Fundamentals*, Addison-Wesley, New Jersey, 1996.
- 23 J. Lee, T. Beechem, T. L. Wright, B. A. Nelson, S. Graham and W. P. King, *J. Microelectromech. Syst.*, 2006, **15**, 1644–1655.
- 24 M. A. Angadi, T. Watanabe, A. Bodapati, X. Xiao, O. Auciello, J. A. Carlisle, J. A. Eastman, P. Keblinski, P. K. Schelling and S. R. Phillpot, *J. Appl. Phys.*, 2006, **99**, 114301–114306.
- 25 O. K. Koo, Y.-S. Liu, S. Shuaib, S. Bhattacharya, M. R. Ladisch, R. Bashir and A. K. Bhunia, *Anal. Chem.*, 2009, **81**, 3094–3101.
- 26 S. Tolnai, *Methods Cell Sci.*, 1975, **1**, 1381–5741.
- 27 C. Laflamme, J. Ho, M. Veillette, M.-C. de Latremaille, D. Verrault, A. Meriaux and C. Duchaine, *Arch. Microbiol.*, 2005, **183**, 107–112.
- 28 <http://probes.invitrogen.com/media/pis/mp01304.pdf>.
- 29 <http://probes.invitrogen.com/media/pis/mp21486.pdf>.
- 30 <http://www.invitrogen.com/site/us/en/home/References/Molecular-Probes-The-Handbook/Nucleic-Acid-Detection-and-Genomics-Technology/Nucleic-Acid-Stains.html>.